



OPEN ACCESS

EDITED BY

Alexandros E. Tsouknidas,
Boston University, United States

REVIEWED BY

Wenxin Niu,
Tongji University, China
Konstantinos Krommydas,
University of Western Macedonia, Greece

*CORRESPONDENCE

Mingzheng Zhang,
✉ zhangmingzheng@jsu.edu.cn

[†]These authors share first authorship

RECEIVED 06 April 2025

ACCEPTED 26 June 2025

PUBLISHED 08 July 2025

CITATION

Zhou X, Qin S, Huang C, Li F, Liu J, Wu T and Zhang M (2025) Biomechanical evaluation of percutaneous cement discoplasty combined with percutaneous vertebroplasty: a finite element analysis.
Front. Bioeng. Biotechnol. 13:1606709.
doi: 10.3389/fbioe.2025.1606709

COPYRIGHT

© 2025 Zhou, Qin, Huang, Li, Liu, Wu and Zhang. This is an open-access article distributed under the terms of the [Creative Commons Attribution License \(CC BY\)](https://creativecommons.org/licenses/by/4.0/). The use, distribution or reproduction in other forums is permitted, provided the original author(s) and the copyright owner(s) are credited and that the original publication in this journal is cited, in accordance with accepted academic practice. No use, distribution or reproduction is permitted which does not comply with these terms.

Biomechanical evaluation of percutaneous cement discoplasty combined with percutaneous vertebroplasty: a finite element analysis

Xu Zhou^{1,2†}, Shenghua Qin^{1,2†}, Chunhai Huang¹, Feiwen Li¹, Jin Liu², Ti Wu² and Mingzheng Zhang^{2*}

¹Department of Orthopaedics, The First Affiliated Hospital of Jishou University, Jishou University, Jishou, China, ²School of Medicine, Jishou University, Jishou, China

Introduction: Since the introduction of percutaneous cement discoplasty (PCD), numerous studies have confirmed its clinical efficacy in elderly patients. However, PCD is also associated with risks such as bone cement leakage and vertebral fractures. The purpose of this study was to present a biomechanical evaluation of two modified versions of PCD performed in combination with percutaneous vertebroplasty (PVP).

Methods: Data from a CT scan of a healthy male's lumbosacral region were used to establish finite element (FE) models of nonsurgical treatment, PCD, L4/5PCD + L4L5PVP (modified technique 1, where the bone cement in the L4/5 disc space does not connect with the L4 and L5 vertebrae) and PCIF (modified technique 2, where the bone cement in the L4/5 disc space connects with the L4 and L5 vertebrae). A compressive preload of 150 N and a moment of 10 N·m were applied to recreate flexion, extension, lateral bending, and axial rotation. The range of motion (ROM) of L3/4 and L4/5, maximum stress on the L3 inferior endplate, L4 inferior endplate and L5 superior endplate, stress on the annulus fibrosus of L4/5, and displacement of the bone cement were evaluated.

Results: Both modified techniques outperformed the simple PCD technique in reducing stress on the endplate, stress on the annulus fibrosus, and displacement of the bone cement. The L4/5PCD + L4L5PVP technique was more advantageous in terms of reducing the incidence of postoperative complications. The addition of the PVP technique significantly enhanced spinal stability by increasing support to adjacent vertebrae, thereby reducing the risk of postoperative endplate fractures and bone cement leakage.

Conclusion: Modified PCD combined with PVP may be a safer and more effective option for treating degenerative disc diseases, providing important references for clinical treatment.

KEYWORDS

spinal degeneration, biomechanics, finite element analysis, percutaneous cement discoplasty, percutaneous vertebroplasty

1 Introduction

With the aging of society, the incidence of spinal degenerative diseases continues to increase. Degenerative disc diseases cause spinal instability which leads to severe back pain and radiating leg pain, significantly diminishing patients' quality of life and increasing the economic burden on families and society (GBD 2015 Disease and Injury Incidence and Prevalence Collaborators, 2016). Conservative treatments have limited efficacy, and traditional open surgeries are often associated with high rates of complications, such as wound infections (Mihailidis et al., 2017). There is an urgent need for new and safe minimally invasive surgical treatments. In 2015, Varga et al. (Varga et al., 2015) were first to report the effectiveness and safety of percutaneous cement discoplasty (PCD) for patients with intractable mechanical back pain and vacuum disc phenomena. This technique involves injecting bone cement into the nucleus of the degenerated disc to maintain the disc height and achieve indirect foraminal decompression, showing promising clinical results (Kiss et al., 2019; Camino et al., 2020). However, because bone cement cannot effectively fuse with the endplate cartilage and has a high elastic modulus, there are risks of postoperative complications such as endplate fractures, implant displacement, and adjacent vertebral fractures (Li et al., 2022; Grewal et al., 2024), which can exacerbate patients' back and leg pain. These issues may stem from insufficient strength of adjacent vertebrae, lumbar instability, and displacement of bone cement within the disc space. Therefore, enhancing the strength of adjacent vertebrae, improving lumbar stability, and securing the bone cement within the disc space are crucial. Hence, we propose performing percutaneous vertebroplasty (PVP) of the adjacent vertebrae above and below the PCD. To achieve this, we propose two modified techniques: technique 1 (L4/5PCD + L4L5PVP, where the bone cement in the L4/5 disc space does not connect with the L4 and L5 vertebrae) or technique 2 (PCIF, where the bone cement in the L4/5 disc space connects with the L4 and L5 vertebrae) to promote fusion of the adjacent spinal motion segments (Xue et al., 2021). These modified techniques aim to reduce the risk of postoperative adjacent vertebral fractures and ensure stable anchoring of the bone cement within the disc space, minimizing the risks of displacement and PCD-related complications, providing a more effective and personalized surgical option for treating degenerative disc diseases and improving patients' quality of life.

2 Methods

2.1 Establishment of the nonsurgical finite element model

CT of a healthy male's lumbosacral region was performed with a slice thickness of 0.63 mm and a resolution of 0.39 mm × 0.39 mm,

Abbreviations: ALL, anterior longitudinal ligament; CL, capsular ligament; FE, finite element; ISL, interspinous ligament; LF, ligamentum flavum; PCD, percutaneous cement discoplasty; PCIF, percutaneous cement interbody fusion; PLL, posterior longitudinal ligament; PVP, percutaneous vertebroplasty; ROM, range of motion; TL, intertransverse ligament; SSL, supraspinous ligament.

resulting in 776 DICOM format images. The lumbar CT images were imported into Mimics 10.01 (Materialise, Belgium) for vertebral segmentation and 3D geometric model reconstruction and exported in STL format. The STL-formatted vertebral models were imported into Geomagic Studio 12.0 (Raindrop Geomagic, Inc., U.S.) for smoothing and surface generation, producing NURBS surfaces, which were exported in IGS format. Since ligaments, such as the anterior longitudinal ligament (ALL), posterior longitudinal ligament (PLL), intertransverse ligament (TL), interspinous ligament (ISL), supraspinous ligament (SSL), capsular ligament (CL), and ligamentum flavum (LF) are not clearly visible in CT images, they were manually drawn as 3D lines in Mimics 10.01. Because the intervertebral disc is a soft tissue, it is difficult to segment from CT images, so it was drawn in CAD software Solidworks 2012 (Dassault Systèmes, France) in accordance with vertebral models and references, with the nucleus pulposus occupying 40% of the disc area (Chen et al., 2001). All the geometric models were imported into ABAQUS 6.11 (Simulia, Inc., USA) to establish the finite element model. The vertebrae consisted of the vertebral body and posterior elements, with the vertebral body further divided into cortical bone, cancellous bone, and the endplate. The cortical bone and endplate were modelled as 0.5 mm thick shell elements, whereas the other bony structures and discs were modelled as solid elements. Ligaments were modelled as two-node truss elements. The material properties were sourced from the literature (Tsuang et al., 2009; Fan et al., 2010; Ambati et al., 2015; Ellingson et al., 2015; Guo et al., 2025) and are detailed in Table 1. The full lumbar finite element model included the L1–L5 vertebrae, sacrum, and connecting discs and ligaments (Figure 1a).

2.2 Establishment of the surgical finite element model

Three surgical models were established: the L4/5 PCD model (Figure 1b), the modified technique 1 (L4/5PCD + L4L5PVP) model (Figure 1c), and the modified technique 2 (PCIF) model (Figure 1d). For the PCD model, the nucleus pulposus in the L4–L5 segment was replaced with bone cement. L4/5PCD + L4L5PVP: In addition to PCD, PVP was performed on the vertebrae above and below the affected disc. PCIF: After windows were created in the endplates above and below the affected disc, PCD was performed, followed by PVP on the adjacent vertebrae. Bone cement was modelled as a solid element with an elastic modulus of 3000 MPa and a Poisson's ratio of 0.3.

2.3 Boundary conditions, model loading, and FE analysis

The facet joints were modelled as sliding friction with a coefficient of 0.1 (Zhong et al., 2009). The contacts between the endplate and vertebral body, the endplate and nucleus pulposus, the endplate and annulus fibrosus, and the bone cement and endplate/cancellous bone were set as tied. The sacrum was fully fixed to simulate the fixation method used in the biomechanical testing of cadaveric samples. A geometric reference point was selected at the

TABLE 1 Material properties of the lumbar finite element model.

Tissue type	Young's modulus (MPa)	Poisson's ratio	Cross-sectional area (mm ²)	Abaqus section type	Abaqus element type
Bony structure					
Cancellous bone	100	0.2	-	Solid	C3D4
Cortical bone	12,000	0.3	-	Shell	S3
Posterior elements	3500	0.25	-	Solid	C3D4
Endplates	3000	0.25	-	Shell	S3
Sacrum and coccyx	3500	0.25	-	Solid	C3D4
Ligaments					
ALL	15	—	40	Truss	T3D2
PLL	10	—	20	Truss	T3D2
SSL	8	—	30	Truss	T3D2
LF	15	—	40	Truss	T3D2
ISL	10	—	40	Truss	T3D2
TL	10	—	1.8	Truss	T3D2
CL	7.5	—	30	Truss	T3D2
Intervertebral disc					
Nuclei pulposi	1	0.499	—	Solid	C3D4
Annuli fibrosi	4.2	0.45	—	Solid	C3D4
Bone cement	3000	0.3	—	Solid	C3D4

centre of the L1 superior surface and coupled to the L1 surface for load application. A compressive preload of 150 N and a moment of 10 N·m were applied to recreate flexion, extension, lateral bending, and axial rotation. The data were collected and analysed post calculation. The evaluation indicators included (1) the ROM of L3/4 and L4/5; (2) the maximum stress on the L3 inferior endplate; (3) the maximum stress on the L4 inferior endplate; (4) the maximum stress on the L5 superior endplate; (5) the maximum displacement of bone cement in the disc space; and (6) the maximum von Mises stress on the L4/5 annulus fibrosus.

3 Results

3.1 FE mesh sensitivity analysis

The maximum von Mises stress on the L4/5 annulus fibrosus was used to perform a mesh sensitivity analysis of the model. The vertebrae of the nonsurgical model were meshed with mesh sizes ranging from 6 mm to 1 mm, and the results were shown in Figure 2. In general, reducing the mesh size improved result accuracy due to enhanced numerical convergence. Under all four loading conditions, the discrepancy in results between the 2-mm and 1-mm meshes was within 5%. After balancing computational efficiency and precision, we ultimately adopted a 2-mm mesh size for the vertebral meshing.

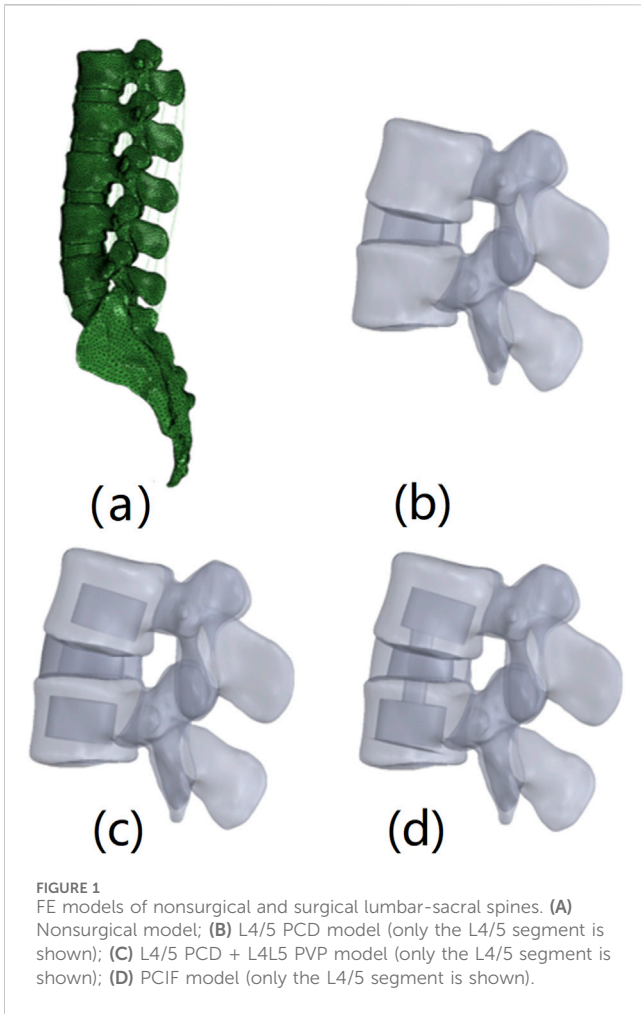
During the meshing process, mesh quality control parameters specified in Table 2 were applied.

3.2 Model validation

To validate the model, the ROM of the L1–L5 vertebrae in the nonsurgical model was compared with that in previous *in vitro* experiments (Yamamoto et al., 1989; Panjabi et al., 1994) and computational models (Chen et al., 2001; Chen et al., 2012; Tsai et al., 2016). As shown in Figure 3, the ROM of the L1–L5 vertebrae in the nonsurgical model was 13.74°, 14.70°, 11.17°, and 10.74° during flexion, extension, lateral bending, and rotation, respectively, showing good consistency with previous results.

3.3 The ROM of the L3/4 and L4/5 segments

In the L4/5PCD model, the L3/4 segment had the lowest ROM in all loading conditions, with values of 1.80° during flexion, 3.94° during extension, 1.68° during lateral bending, and 2.75° during rotation. The ROM of the segments in all loading conditions was similar in the L4/5PCD + L4L5PVP and PCIF models (Figure 4a; Table 3). The ROM of the L4/5 segment in all loading conditions was greater in the L4/5PCD model than in the L4/5PCD + L4L5PVP and PCIF models, with values



of 1.38° during flexion, 2.72° during extension, 1.16° during lateral bending, and 0.28° during rotation (Figure 4b; Table 3).

3.4 Maximum von mises stress on the endplates

The maximum von Mises stress on the L3 and L4 inferior endplates and the L5 superior endplate in all four loading conditions was lowest in the L4/5PCD + L4L5PVP model; however, the von Mises stress on the L5 superior endplate during lateral bending was greater in the L4/5PCD + L4L5PVP model than in the PCIF model. The differences between the L4/5PCD + L4L5PVP and PCIF models were minimal (Figures 5; Table 3).

3.5 Maximum von mises stress on the L4/5 annulus fibrosus

The maximum stress on the L4/5 annulus fibrosus in all four loading conditions was lower in both models than in the PCD model. L4/5PCD + L4L5PVP resulted in the lowest stress, with 0.1399 MPa during flexion, 0.6461 MPa during extension, 0.3297 MPa during lateral bending, and 0.1003 MPa during rotation (Figure 6; Table 3).

3.6 Bone cement displacement

The maximum displacement of bone cement in the disc space during flexion, extension, and lateral bending was similar in all four loading conditions in the L4/5PCD and PCIF models. However, PCIF significantly reduced displacement during rotation. L4/5PCD + L4L5PVP resulted in the smallest displacement (Figure 7; Table 3).

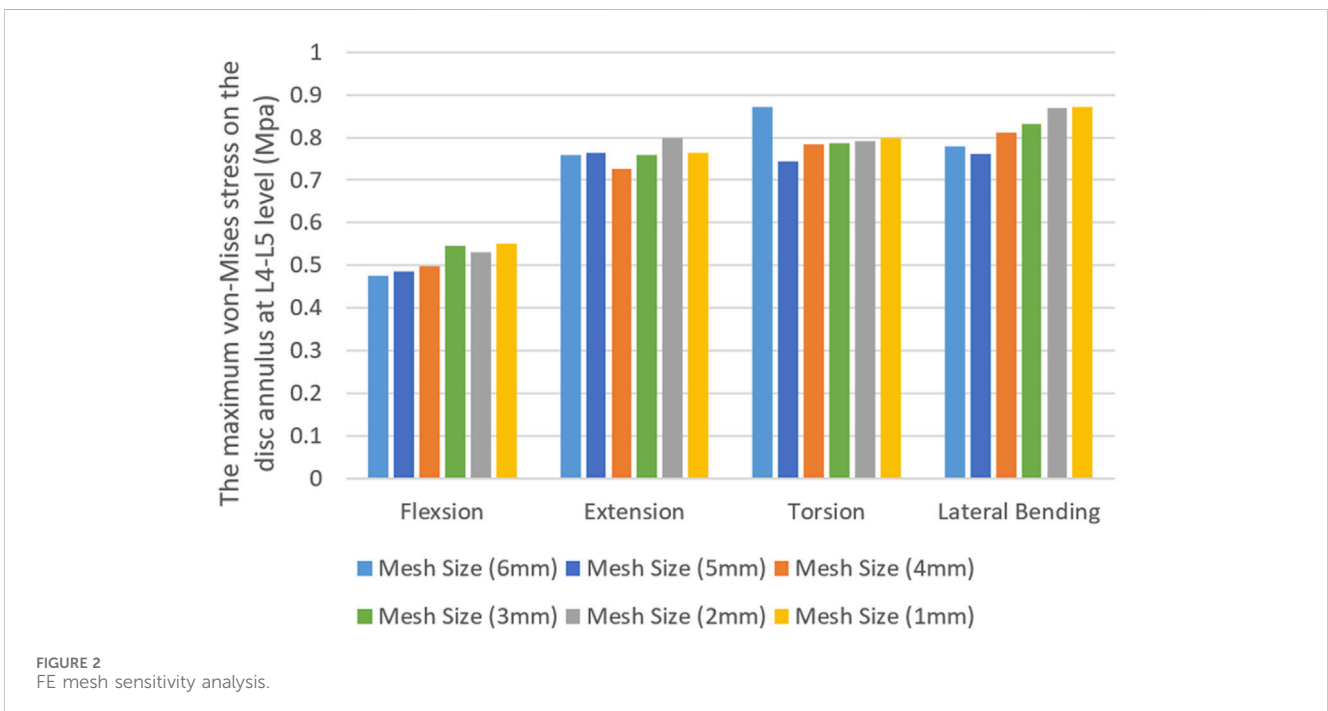
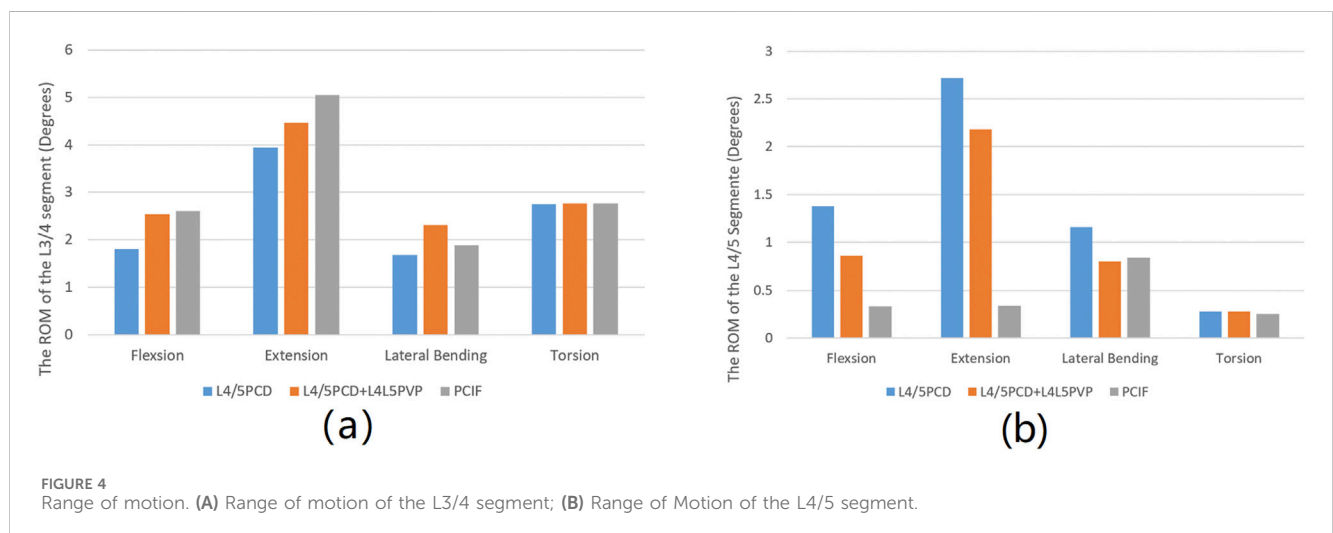
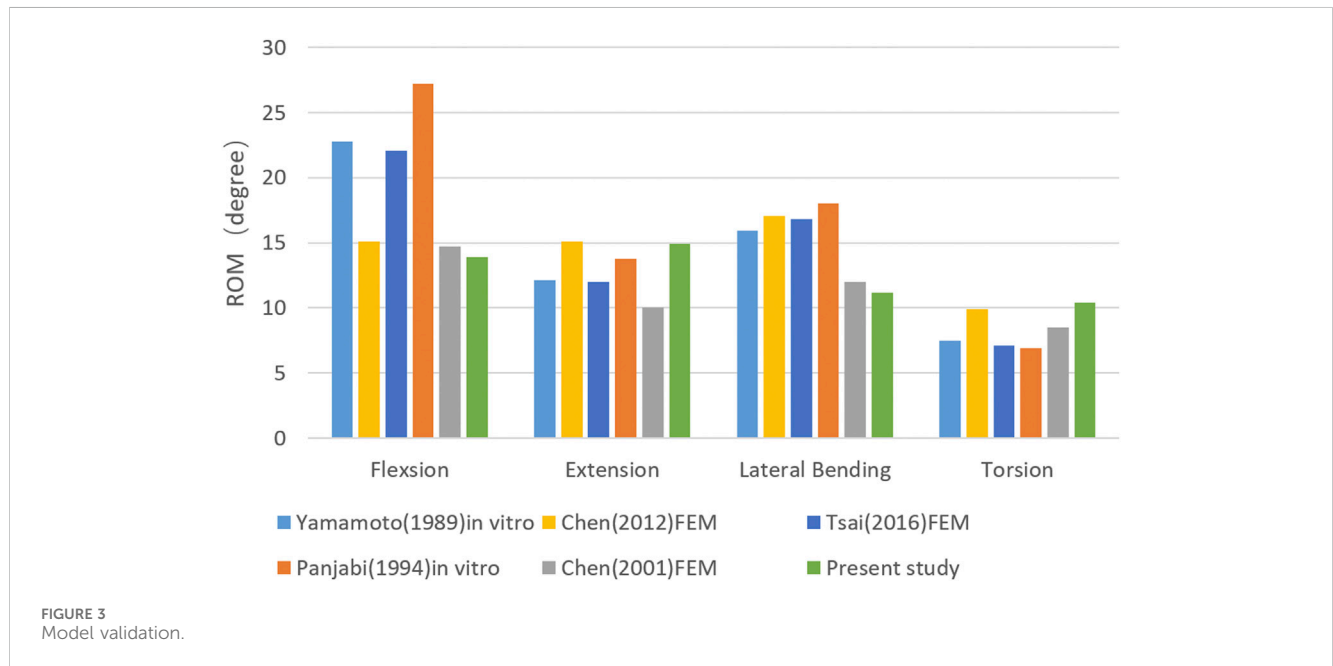


TABLE 2 Quality control parameters of the FE meshes.

Quality control parameters	Quadrilateral element	Triangular element	Tetrahedral element
Aspect ratio	<5.0	<5.0	<5.0
Jacobian ratio	>0.7	>0.7	>0.7
Internal angles	45°–135°	20°–120°	20°–120°



4 Discussion

Since the introduction of PCD, numerous studies have explored its effectiveness (Willhuber et al., 2021; Jia et al., 2022; Li et al., 2022; Techens et al., 2022; Zhang et al., 2024) and subsequently confirmed its clinical efficacy in elderly patients with vacuum disc phenomena

and lumbar instability. However, PCD is associated with risks such as bone cement leakage and vertebral fractures (Kiss et al., 2019; Camino-Willhuber et al., 2021; Yamada et al., 2021). After PCD, the bone cement acts as an independent disc spacer but cannot fully fuse with the endplate cartilage. The annulus fibrosus, which is often incomplete or weak, may be further damaged during surgery,

TABLE 3 Analysis results comparison table.

FE models	Loading conditions	ROM (°)		Maximum von mises stress (MPa)				Bone cement displacement (mm)
		L3/ 4 segment	L4/ 5 segment	L3 inferior endplate	L4 inferior endplate	L5 superior endplate	L4/5 annulus fibrosus	
L4/5 PCD	Flexion	1.80	1.38	30.90	25.61	20.50	0.24	2.71
	Extension	3.94	2.72	54.82	53.66	46.96	0.65	4.64
	Lateral bending	1.68	1.16	27.51	26.59	27.86	0.33	1.12
	Torsion	2.75	0.28	16.17	20.10	23.13	0.13	4.53
L4/5 PCD + L4L5 PVP	Flexion	2.54	0.86	29.41	12.35	14.18	0.14	1.81
	Extension	4.46	2.18	47.76	24.25	29.32	0.33	1.82
	Lateral bending	2.31	0.80	26.65	15.31	21.82	0.22	0.88
	Torsion	2.77	0.28	15.79	15.53	18.62	0.10	0.86
PCIF	Flexion	2.60	0.33	30.60	21.90	20.76	0.21	2.54
	Extension	5.05	0.34	51.67	36.65	44.16	0.51	4.70
	Lateral bending	1.89	0.84	27.21	23.23	17.66	0.27	1.01
	Torsion	2.76	0.25	16.48	17.09	19.42	0.11	1.60

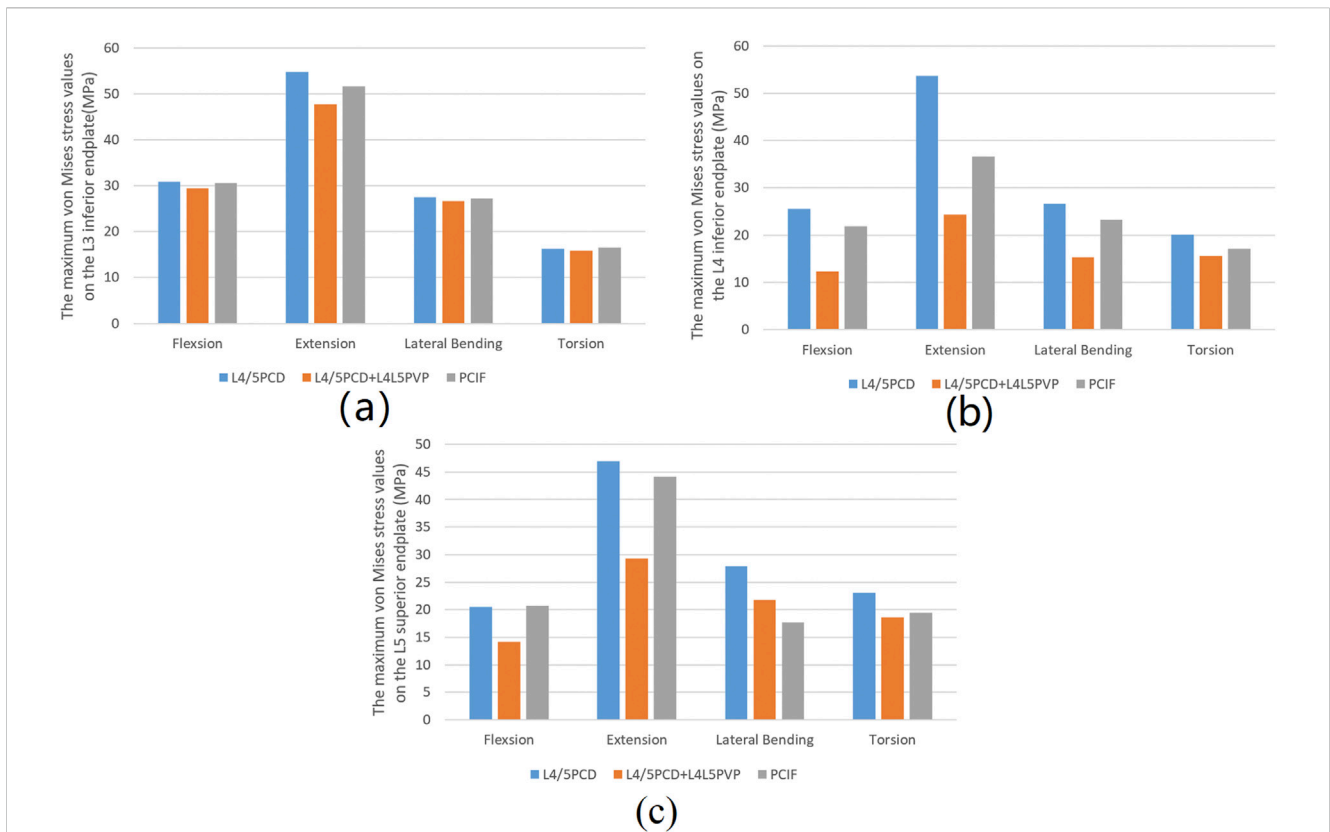


FIGURE 5 Maximum von Mises stress values. **(A)** Maximum von Mises stress values on the inferior endplate of L3; **(B)** Maximum von Mises stress values on the inferior endplate of L4; **(C)** Maximum von Mises stress values on the superior endplate of L5.

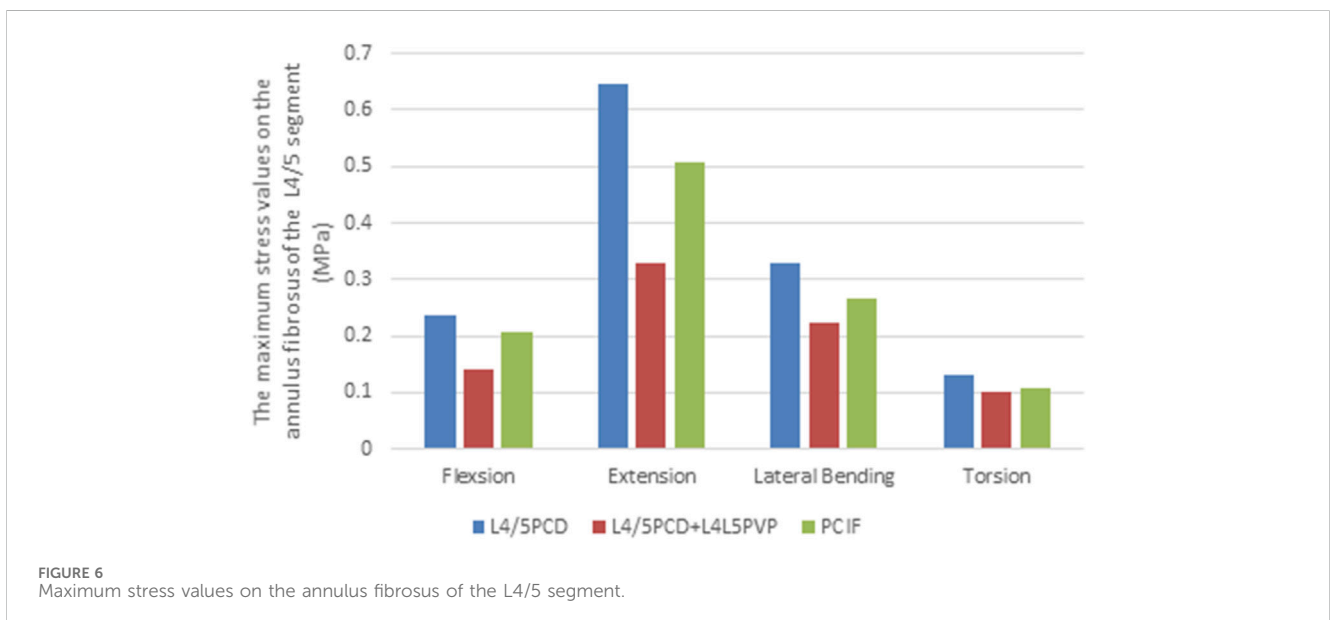


FIGURE 6 Maximum stress values on the annulus fibrosus of the L4/5 segment.

increasing the risk of cement leakage and displacement, similar to cage displacement in lumbar fusion surgery. Instability and osteoporosis progression after PCD are significant factors contributing to cement displacement (Kimura et al., 2012; Lee

et al., 2018; Park et al., 2019). PCD does not provide sufficient stability or achieve solid interbody fusion, making cement displacement a critical concern. In this study, L4/5PCD + L4L5PVP resulted in the smallest degree of cement displacement,

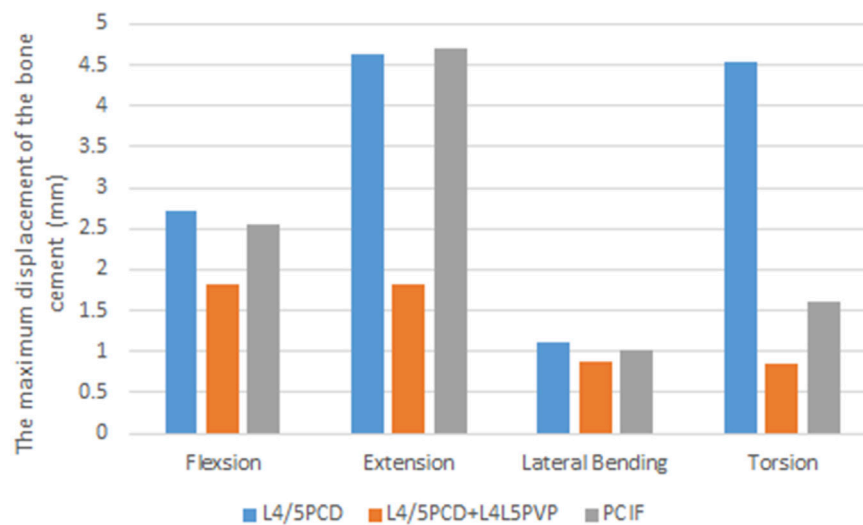


FIGURE 7
The maximum displacement of the bone cement.

indicating its efficacy for securing the cement. The addition of the PVP technique enhances support to adjacent vertebrae, effectively securing the cement and reducing the risk of implant displacement.

Techens et al. (2020) reported the stress concentration on the endplates adjacent to the PCD-treated discs in an *in vitro* biomechanical study, which was consistent with the stress concentration calculated in a sheep model examined by Ghandour et al. (2022). To address the risk of adjacent endplate fractures, we compared the maximum stress on the L3 inferior endplate, L4 inferior endplate, and L5 superior endplate between PCD and the two modified techniques. Compared with PCD, both L4/5PCD + L4L5PVP and PCIF reduced the maximum stress on the L3 inferior endplate, indicating that reinforcement provided by PVP does not increase the risk of adjacent vertebral fractures. This advantage stems from the ability of PVP to distribute stress, reduce the burden on the endplates and lower the risk of postoperative fractures.

The ROM of the L3/4 segment was the lowest in the L4/5PCD model, indicating the strongest restriction on spinal motion, likely due to the high elastic modulus of the disc after cement injection. The ROM of the L4/5 segment in the L4/5PCD model was higher, indicating limited improvement in stability. In contrast, L4/5PCD + L4L5PVP and PCIF significantly reduced ROM, with PCIF providing the strongest stability as it fuses adjacent vertebrae and the cement in the affected disc space, reducing the risk of adjacent vertebral fractures and cement displacement. Li et al. (2022) also used finite element analysis to study PCD, confirming its impact on lumbar ROM and strength. The fusion of bone cement with endplates offers more biomechanical advantages, reducing the risk of cement subsidence and improving segmental stability.

The analysis of stress on the annulus fibrosus revealed that, compared with PCD, both L4/5PCD + L4L5PVP and PCIF reduced the maximum stress on the L4–5 annulus fibrosus in all motion directions, with L4/5PCD + L4L5PVP showing the best results. This finding indicates that the addition of PVP led to effective stress distribution, reducing the burden on the annulus fibrosus and lowering the risk of postoperative annulus rupture.

Although the biomechanical effects of PCD and the two modified techniques were compared via finite element analysis, several limitations should be noted. For example, single subject CT images were used, thus limiting the generalizability of the results. A larger sample of patients of different sexes, ages, and weights should be selected for future studies to improve the applicability of the findings. In terms of model construction, simplified material parameters were used: the ligaments were modelled as two-node truss elements, while annulus fibrosi and endplates were modelled as isotropic linear elastic materials. The above simplifications may not accurately capture the complex kinematic characteristics of the spine. Muscular contributions were not incorporated in the simulation, and the study exclusively focused on static analyses without dynamic simulations. Subsequent studies ought to overcome these limitations by developing more refined models, such as utilizing three-dimensional solid ligaments with nonlinear properties to simulate ligaments and incorporating dynamic loading simulations to capture time-dependent behaviours. Furthermore, in future research, clinical follow-up data should be included to further validate the accuracy and reliability of the finite element analysis results.

5 Conclusion

In conclusion, both L4/5PCD + L4L5PVP and PCIF outperformed PCD in reducing the maximum stress on the endplate, maximum stress on the annulus fibrosus, and maximum bone cement displacement. Compared with PCIF, L4/5PCD + L4L5PVP was associated with fewer postoperative complications. The use of these techniques together enhance spinal stability by increasing support to adjacent vertebrae, which reduces the risk of postoperative complications. For patients with degenerative disc diseases, especially elderly patients, the combination of these techniques may be a safer and more effective treatment option, providing important references for clinical treatment.

Data availability statement

The raw data supporting the conclusion of this article will be made available by the authors, without undue reservation.

Author contributions

XZ: Data curation, Formal Analysis, Funding acquisition, Investigation, Writing – original draft. SQ: Data curation, Formal Analysis, Funding acquisition, Investigation, Validation, Writing – original draft. CH: Data curation, Formal Analysis, Resources, Supervision, Writing – review & editing. FL: Data curation, Formal Analysis, Resources, Supervision, Writing – review & editing. JL: Formal Analysis, Software, Visualization, Writing – review & editing. TW: Software, Visualization, Writing – review & editing. MZ: Conceptualization, Funding acquisition, Methodology, Project administration, Software, Supervision, Validation, Writing – review & editing.

Funding

The author(s) declare that financial support was received for the research and/or publication of this article. This work was supported

References

- Ambati, D. V., Wright, E. J., Lehman, R. J., Kang, D. G., Wagner, S. C., and Dmitriev, A. E. (2015). Bilateral pedicle screw fixation provides superior biomechanical stability in transforaminal lumbar interbody fusion: a finite element study. *Spine J.* 15 (8), 1812–1822. doi:10.1016/j.spinee.2014.06.015
- Camino, W. G., Kido, G., Pereira, D. M., Estefan, M., Bendersky, M., Bassani, J., et al. (2020). Percutaneous cement discoplasty for the treatment of advanced degenerative disc conditions: a case series analysis. *Glob. Spine J.* 10 (6), 729–734. doi:10.1177/2192568219873885
- Camino-Willhuber, G., Norotte, G., Bronsard, N., Kido, G., Pereira-Duarte, M., Estefan, M., et al. (2021). Percutaneous cement discoplasty for degenerative low back pain with vacuum phenomenon: a multicentric study with a minimum of 2 years of Follow-Up. *World Neurosurg.* 155, e210–e217. doi:10.1016/j.wneu.2021.08.042
- Chen, C. S., Cheng, C. K., Liu, C. L., and Lo, W. H. (2001). Stress analysis of the disc adjacent to interbody fusion in lumbar spine. *Med. Eng. Phys.* 23 (7), 485–493. doi:10.1016/S1350-4533(01)00076-5
- Chen, S. H., Lin, S. C., Tsai, W. C., Wang, C. W., and Chao, S. H. (2012). Biomechanical comparison of unilateral and bilateral pedicle screws fixation for transforaminal lumbar interbody fusion after decompressive surgery—a finite element analysis. *BMC Musculoskelet. Disord.* 13, 72. doi:10.1186/1471-2474-13-72
- Ellingson, A. M., Shaw, M. N., Giambini, H., and An, K. (2015). Comparative role of disc degeneration and ligament failure on functional mechanics of the lumbar spine. *Comput. Methods Biomechanics Biomed. Eng.* 19 (9), 1009–1018. doi:10.1080/10255842.2015.1088524
- Fan, C. Y., Hsu, C. C., Chao, C. K., Lin, S. C., and Chao, K. H. (2010). Biomechanical comparisons of different posterior instrumentation constructs after two-level ALIF: a finite element study. *Med. Eng. Phys.* 32 (2), 203–211. doi:10.1016/j.medengphy.2009.12.002
- GBD 2015 Disease and Injury Incidence and Prevalence Collaborators (2016). Global, regional, and national incidence, prevalence, and years lived with disability for 310 diseases and injuries, 1990–2015: a systematic analysis for the Global Burden of Disease Study 2015. *Lancet* 388 (10053), 1545–1602. doi:10.1016/S0140-6736(16)31678-6
- Ghandour, S., Pazarlis, K., Lewin, S., Isaksson, P., Försth, P., and Persson, C. (2022). An ex-vivo model for the biomechanical assessment of cement discoplasty. *Front. Bioeng. Biotechnol.* 10, 939717. doi:10.3389/fbioe.2022.939717
- Grewal, S. S., Hirsch, J. A., Cancelliere, N. M., Ghozy, S., Pereira, V. M., and Dmytriw, A. A. (2024). Efficacy and safety of percutaneous cement discoplasty in the management

by the scientific research start-up funds of Jishou University for the introduction of talent (2024–12), the Natural Science Foundation of Hunan Province(2025JJ70608) and the scientific research projects of Jishou University (Jdzd22015, Jdy23081).

Conflict of interest

The authors declare that the research was conducted in the absence of any commercial or financial relationships that could be construed as a potential conflict of interest.

Generative AI statement

The author(s) declare that no Generative AI was used in the creation of this manuscript.

Publisher's note

All claims expressed in this article are solely those of the authors and do not necessarily represent those of their affiliated organizations, or those of the publisher, the editors and the reviewers. Any product that may be evaluated in this article, or claim that may be made by its manufacturer, is not guaranteed or endorsed by the publisher.

of degenerative spinal diseases: a systematic review and meta-analysis. *Neuroradiol. J.* 37 (4), 434–440. doi:10.1177/19714009231212368

Guo, W., Wang, Z., Song, M., Yang, W., Zhang, H., Yang, W., et al. (2025). Biomechanical evaluation of oblique lateral interbody fusion with various fixation methods for degenerative lumbar scoliosis: a finite element analysis considering different bone densities. *Front. Bioeng. Biotechnol.* 13, 1562268. doi:10.3389/fbioe.2025.1562268

Jia, H., Xu, B., and Qi, X. (2022). Biomechanical evaluation of percutaneous cement discoplasty by finite element analysis. *BMC Musculoskelet. Disord.* 23, 594. doi:10.1186/s12891-022-05508-1

Kimura, H., Shikata, J., Odate, S., Soeda, T., and Yamamura, S. (2012). Risk factors for cage retropulsion after posterior lumbar interbody fusion: analysis of 1070 cases. *Spine* 37 (13), 1164–1169. doi:10.1097/brs.0b013e318257f12a

Kiss, L., Varga, P. P., Szoverfi, Z., Jakab, G., Eltes, P. E., and Lazary, A. (2019). Indirect foraminal decompression and improvement in the lumbar alignment after percutaneous cement discoplasty. *Eur. Spine J.* 28 (6), 1441–1447. doi:10.1007/s00586-019-05966-7

Lee, D., Park, Y., Song, S., Jeong, S., and Kim, D. (2018). Risk factors for posterior cage migration after Lumbar interbody fusion surgery. *Asian Spine J.* 12 (1), 59–68. doi:10.4184/asj.2018.12.1.59

Li, S., Shao, P., Xu, B., Liu, Y., Zhang, J., Liu, G., et al. (2022). Biomechanical evaluation of effects of percutaneous cement discoplasty and percutaneous cement interbody fusion on spinal stability. *Zhongguo Xiu Fu Chong Jian Wai Ke Za Zhi* 36 (11), 1407–1412. doi:10.7507/1002-1892.202206052

Li, S., Xu, B., Liu, Y., Zhang, J., Xu, G., Shao, P., et al. (2022). Biomechanical evaluation of spinal column after percutaneous cement discoplasty: a finite element analysis. *Orthop. Surg.* 14 (8), 1853–1863. doi:10.1111/os.13314

Mihailidis, H. G., Manners, S., Churilov, L., and Quan, G. (2017). Is spinal surgery safe in octogenarians? *ANZ J. Surg.* 87 (7-8), 605–609. doi:10.1111/ans.13885

Panjabi, M. M., Oxland, T. R., Yamamoto, I., and Crisco, J. J. (1994). Mechanical behavior of the human lumbar and Lumbosacral spine as shown by three-dimensional load-displacement curves. *J. Bone Jt. Surg. Am.* 76 (3), 413–424. doi:10.2106/00004623-199403000-00012

Park, M. K., Kim, K. T., Bang, W. S., Cho, D. C., Sung, J. K., Lee, Y. S., et al. (2019). Risk factors for cage migration and cage retropulsion following transforaminal lumbar interbody fusion. *Spine J.* 19 (3), 437–447. doi:10.1016/j.spinee.2018.08.007

- Techens, C., Eltes, P. E., Lazary, A., and Cristofolini, L. (2022). Critical review of the state-of-the-art on lumbar percutaneous cement discoplasty. *Front. Surg.* 9, 902831. doi:10.3389/fsurg.2022.902831
- Techens, C., Palanca, M., Eltes, P. E., Lazary, Á., and Cristofolini, L. (2020). Testing the impact of discoplasty on the biomechanics of the intervertebral disc with simulated degeneration: an in vitro study. *Med. Eng. Phys.* 84, 51–59. doi:10.1016/j.medengphy.2020.07.024
- Tsai, P. I., Hsu, C. C., Chen, S. Y., Wu, T. H., and Huang, C. C. (2016). Biomechanical investigation into the structural design of porous additive manufactured cages using numerical and experimental approaches. *Comput. Biol. Med.* 76, 14–23. doi:10.1016/j.compbiomed.2016.06.016
- Tsung, Y. H., Chiang, Y. F., Hung, C. Y., Wei, H. W., Huang, C. H., and Cheng, C. K. (2009). Comparison of cage application modality in posterior lumbar interbody fusion with posterior instrumentation--a finite element study. *Med. Eng. Phys.* 31 (5), 565–570. doi:10.1016/j.medengphy.2008.11.012
- Varga, P. P., Jakab, G., Bors, I. B., Lazary, A., and Szövérfi, Z. (2015). Experiences with PMMA cement as a stand-alone intervertebral spacer: percutaneous cement discoplasty in the case of vacuum phenomenon within lumbar intervertebral discs. *Orthopade* 44, S1–S7.
- Willhuber, G. O. C., Bendersky, M., Viltz, C., Kido, G., Pereira Duarte, M., Estefan, M., et al. (2021). Accuracy of intraoperative neuromonitoring during percutaneous cement discoplasty. *Rev. la Fac. Ciencias Médicas Córdoba* 78 (3), 257–263.
- Xue, Y. D., Zhang, Z. C., and Dai, W. X. (2021). Investigation of preoperative traction followed by percutaneous kyphoplasty combined with percutaneous cement discoplasty for the treatment of severe thoracolumbar osteoporotic vertebral compression fractures. *Int. J. Gen. Med.* 14, 6563–6571. doi:10.2147/ijgm.s333532
- Yamada, K., Nakamae, T., Nakanishi, K., Kamei, N., Hiramatsu, T., Okuda, T., et al. (2021). Long-term outcome of targeted therapy for low back pain in elderly degenerative lumbar scoliosis. *Eur. Spine J.* 30 (7), 2020–2032. doi:10.1007/s00586-021-06805-4
- Yamamoto, I., Panjabi, M. M., Crisco, T., and Oxland, T. (1989). Three-dimensional movements of the whole lumbar spine and lumbosacral joint. *Spine* 14 (11), 1256–1260. doi:10.1097/00007632-198911000-00020
- Zhang, H., Gao, J., and Tang, X. (2024). Percutaneous cement discoplasty for the treatment of lumbar degenerative diseases: a system review and meta-analysis. *Medicine* 103 (34), e39345. doi:10.1097/md.00000000000039345
- Zhong, Z. C., Chen, S. H., and Hung, C. H. (2009). Load- and displacement-controlled finite element analyses on fusion and non-fusion spinal implants. *Proc. Inst. Mech. Eng. H.* 223 (2), 143–157. doi:10.1243/09544119jeim476